Research Article

Biosynthesis of Silver Nanoparticles using *Myrmecodia* sp. Bulb Extract: *in vivo* Wound Healing Potency in *Mus musculus* L.

Retno Aryani*
Animal Anatomy and Microtechnique Laboratory, Department of Biology, Faculty of Mathematics and Natural Sciences Mulawarman University, Kalimantan Timur, Indonesia

Misra Wati, Erin Maytari and Rudy Agung Nugroho
Animal Physiology, Development, and Molecular Laboratory, Department of Biology, Faculty of Mathematics and Natural Sciences Mulawarman University, Kalimantan Timur, Indonesia

Hetty Manurung
Plant Physiology and Development Laboratory, Department of Biology, Faculty of Mathematics and Natural Sciences Mulawarman University, Kalimantan Timur, Indonesia

Rudianto Rudianto
Postgraduate student of Department of Biology, Faculty of Mathematics and Natural Sciences Mulawarman University, Kalimantan Timur, Indonesia

* Corresponding author. E-mail: retnoaryani@fmipa.unmul.ac.id   DOI: 10.14416/j.asep.2025.06.003

Abstract
Myrmecodia sp. is a plant species often used in conventional medicine for its anti-inflammatory, anticancer, and wound recovery activities. This study was to determine the wound healing properties of AgNPs produced using bulb extracts of *Myrmecodia* sp. (M-AgNPs). M-AgNPs were synthesized by adding 100 mL of a 1 mM aqueous solution of silver nitrate to 100 mL of a 0.1% ethanolic bulb extract of *Myrmecodia* sp. The M-AgNPs experiment was characterized by visible changes in color, UV–VIS spectroscopy, scanning electron microscopy (SEM), X-ray diffraction (XRD), and Fourier transform infrared (FTIR) spectroscopy. The present study used mice to conduct an in vivo examination of wound healing. The results showed a color transition from a dark brown hue to a lighter pale brown shade and a 460 nm peak in the UV-visible spectrum, indicating M-AgNP synthesis. Several possible wound-healing chemicals for M-AgNPs were identified (FTIR and XRD). The morphology of the M-AgNPs was mostly nanocubes (with average size of 805 nm). Mouse wounds treated with 20% M-AgNPs showed enhanced healing rates and reduced levels of proteins, DNA, and hydroxyproline. Histopathological wounds treated with M-AgNPs had notably elevated fibroblast counts. M-AgNPs-treated mice exhibited a notable enhancement in wound recovery, suggesting eco-friendly practices of M-AgNPs in wound medicine.

Keywords: Mice, *Myrmecodia* sp., Nanoparticle, Topical ointment, Wound treatment

1 Introduction

Nanobiotechnology, which focuses on creating nanoscale particles, has shown great promise in the fields of medicine [1] and healthcare [2]. Submicron particles possess distinct structural, biological, and spectral characteristics, providing several benefits for a range of applications including medication delivery, biosensors, cell proliferation, and wound healing [3]. Metal nanoparticles, particularly titanium, iron,

magnesium, zinc, and silver nanoparticles, exhibit diverse forms and functions.

The advent of nanotechnology has enabled environmentally friendly manufacturing of silver nanoparticles (AgNPs), presenting a new possible therapeutic approach. Chemical methods remain the predominant approach for synthesizing AgNPs because of their straightforward preparation, despite the existence of other alternatives [4]. However, chemical procedures require the use of a multitude of toxic reagents [5]. Moreover, alternative traditional procedures are expensive, labor intensive, and produce waste that is detrimental to the environment and living beings. Some biological methods, such as the use of plant extracts, Streptomyces, bacteria, fungi, and algae, are regarded as ecologically sustainable, healthy, and non-toxic. Nonetheless, the preservation of hygienic culture conditions and an aseptic atmosphere is essential for treatments involving microorganisms, which are somewhat intricate [6].

The plant-based biosynthesis of AgNPs is straightforward and economical compared to other biological methods. Phytochemical substances, including phenols, flavonoids, alkaloids, and terpenoids, can efficiently convert metallic ions to metallic nanoparticles in a one-step process without the need for additional chemical agents [7]. The biomolecules in the plant extract markedly alter the distribution and size of the metal nanoparticles, thereby influencing the physical, chemical, and biological properties of the synthesized nanoparticles. Several biological applications of AgNPs have been reported in recent years, particularly for wound healing therapies [8]. The application of phytotherapeutics has increased in recent years, mostly owing to their perceived efficacy and absence of detrimental side effects.

Myrmecodia sp., often known as an ant nest plant, is an epiphytic flora that exhibits significant antioxidant capacity [9]. The ant nest plant is a member of the Hydnophytinae subfamily within the Rubiaceae family, which includes five genera. Sudiono *et al.*, [10] described *Myrmecodia* sp. as a plant with symbiotic interactions with ants, and therapeutic characteristics. Ant nest plants contain beneficial substances, including vitamins, minerals, glycosides, polyphenols, tocopherols, flavonoids, and tannins [11]. These chemicals possess a plethora of potent antioxidant and medicinal actions [12]. Traditional medicine has long made use of the ant nest plant, which may be found in several regions of Indonesia (e.g., Papua and Kalimantan), to aid in the healing process after giving birth and during nursing [11], as well as its potential as a wound healing agent.

Wound formation occurs as a result of the disruption of the histological structure of skin tissue caused by various internal or external sources, or the progressive impairment of any layer of the skin, ultimately leading to tissue disturbance [13]. The presence of wounds facilitates the infiltration of various microbiological agents, such as bacteria, viruses, and foreign substances, into the human body. Skin wound inflammation can be attributed to localized microbial infections. Additionally, it is worth noting that microbial infection, which is a broad systemic infection, may be a potentially life-threatening illness [14]. Therefore, it is important to conduct further studies to ascertain uncomplicated and efficacious methods for correct management and healing of cutaneous injuries. The primary objectives include cessation of hemorrhage, eradication of microbial contamination in wounds, and facilitation of optimal wound healing without any untoward outcomes or anatomical abnormalities [15].

Moreover, AgNPs have been shown to possess promising wound-healing properties. Several studies have found that the use of silver nanoparticles (AgNPs) biosynthesized by *Azadirachta indica* [16] and *Cotoneaster nummularia* [17] improves wound healing by controlling various processes in wound healing, growth factors, and cytokines via their antibacterial and anti-inflammatory properties. Another study discovered that AgNPs had an impact on the maturation of different types of cells and numerous structures involved in wound healing, as shown by histopathological examination [18]. AgNPs from *Azadirachta indica* (AAgNPs) and *Catharanthus roseus* (CAgNPs) leaf extracts resulted in faster wound healing, higher collagen deposition, and increased DNA and protein content in wounds treated with AAgNPs and CAgNPs (at a concentration of 1% w/w) compared to the control and vehicle control wounds of BALB/c mice. These results validate the potential use of AgNPs in therapeutic applications, particularly as agents for promoting wound healing. Therefore, it is necessary to obtain a more comprehensive understanding and investigate the impact of plant-derived AgNPs made from plants on wound healing.

Although studies on green synthesis using plant extracts are well documented, the efficacy of AgNPs generated from the bulb extract of *Myrmecodia* sp. for

wound healing has not been investigated. This study evaluated the biogenic synthesis of silver nanoparticles (AgNPs) using *Myrmecodia* sp. bulb extract for in vivo wound healing. Furthermore, the study innovation involves eco-friendly synthesis and enhanced in vivo wound-healing performance.

2 Materials and Methods

The present flowchart of the method is an outline of the experimental design of the study (Figure 1).
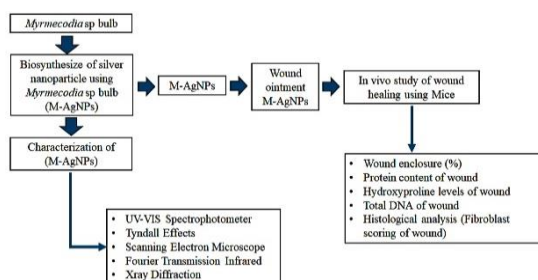
Figure 1: The mind map of the study of silver nanoparticle derived from *Myrmecodia* sp. bulb for wound healing in mice.

2.1 *Myrmecodia sp. Bulb extract preparation*

Myrmecodia sp. bulbs were purchased from a local agriculturist in East Kalimantan, Indonesia. Bulbs were identified using a plant reference handbook. The desiccated bulb was diced into tiny fragments and pulverized using a motorized blender. One kilogram of bulb powder was mixed with 10 liters of 96% ethanol. The solution was agitated daily for 15 min. Following a two-day soaking period, the material was filtered using filter paper, yielding a residue and filtrate. The residue was soaked again in 10 L 96% ethanol for 2 days. All the filtrates that had been obtained from the maceration process were mixed. The filtrate was evaporated using a rotary evaporator at 60 °C until total removal of ethanol was achieved. The concentrated filtrate was stored at 4 °C until further use.

2.2 *Biosynthesis of M-AgNPs*

The biogenesis of M-AgNPs was conducted using 1 mM AgNO₃, according to the protocol described by Maarebia *et al*., [19]. The ethanolic bulb extract (20 g) was combined with 200 mL of 96% ethanol (1:10 ratio),

followed by the addition of 2000 mL of 1 mM AgNO₃ solution (1:10 ratio). The mixture was homogenized and incubated at 70 °C for 30 h, after which it was evaporated using a rotary evaporator. The synthesis of M-AgNPs was evaluated by colorimetric changes and the Tyndall effect [20].

2.3 *Characterization of M-AgNPs*

The presence of M-AgNPs was verified using a UV-Vis spectrophotometer (Shimadzu, UV-1280, Japan) over a wavelength range of 350–750 nm. Scanning Electron Microscopy (SEM; SU 3500, Hitachi, Europe, 26 kV and 50,000 × magnification) was used to visualize the surface morphology of M-AgNPs. X-ray diffraction (XRD; Bruker D8, Blue Scientific, USA) at λ = 1.54056 Å, 40 kV, and 35 mA was used to assess the chemical composition of M-AgNPs. To analyze the phytochemicals present in the vicinity of the M-AgNPs, Fourier transform infrared (FTIR) spectroscopy (Agilent Cary 630 USA) was conducted as described by Barabadi *et al*., [21].

2.4 *Wound ointment preparation*

To prepare the wound ointment, ethanolic bulb extracts of *Myrmecodia* sp., M-AgNPs, and Vaseline were prepared and mixed according to the formulations shown in Table 1. Vaseline was melted on a hot plate, and either the ethanolic bulb extract of *Myrmecodia* sp. or M-AgNPs was added. The mixture was stirred until homogeneous and placed in an ointment pot [22].

Table 1: Wound ointment formula using M-AgNPs and Vaseline.

Ingredients	M-AgNPs (%)		
	10	**20**	**30**
Myrmecodia sp. ethanolic bulb extract or M-AgNPs (g)	3	6	9
Vaseline (g)	27	24	21
Total (g)	30	30	30

2.5 *In vivo study*

2.5.1 *Mice preparation and treatment*

In total, 72 male mice (Three-month age, initial body weight of ±20 g) obtained from a mouse farm in Samarinda, Indonesia were selected as test animals. Mice were divided into nine groups, namely three control groups (K- = wound incision without any

treatment; K+Vas = wound incision with Vaseline treatment; and K+Pov = wound incision with povidone iodine treatment) and six treatment groups: P1-3 (wound incision with wound ointment of bulb ethanolic extract of *Myrmecodia* sp. at concentrations of 10, 20, and 30%) and P4-6 (wound incision with wound ointment of M-AgNPs at concentrations of 10, 20%, and 30%). Each group consisted of eight mice. All mice were acclimatized to the research facility for seven days with feed and water ad libitum.

The mice were anesthetized using 10% ketamine to create wounds. An amount of 0.2 mL ketamine solution was injected intramuscularly. After 3 min, the back of each mouse was shaved until the skin was visible and cleaned with 70% alcohol. A wound (1 cm long and 1 mm deep) was made using a sterile scalpel. The wounds were treated according to group from day 0 to day 15. Wound enclosure measurements were performed every three days using a digital caliper on days 0, 3, 6, 9, 12, and 15. Wound data were recorded, and wound conditions were documented using a digital camera.

The data obtained by measuring the incision wound every three days were calculated as the percentage of wound enclosure using the following formula [23]:

$$Px = \frac{(p^2)-(px^2)}{(p^2)} \times 100\%$$

Where:
Px: day-x wound closure percentage
p: day 0 wound length
px: day x wound length

Dissection of the test animals and collection of skin tissue was performed on day 10 after wound ointment treatment, as indicated by groups of mice showing 100% wound enclosure. Furthermore, four mice with the most healed wounds were anesthetized. The skin tissue in the wound area was taken and divided into 4 parts weighing 0.05 g for each. The first part was added to 200 µL of 4% NaCl for the protein content measurement. The second part was mixed with 200 µL of PBS for total DNA measurements. The third part was incubated at 60 °C overnight to measure hydroxyproline levels, and the last part was prepared for histological analysis by adding 10% NBF.

2.5.2 Protein content measurement

Protein levels in wound tissue samples were measured using the Lowry method [24]. Wound skin tissue samples (0.05 g) were taken from the wound area, placed into a tube containing 200 µL of 4% NaCl, and homogenized (Beadbug Microtube Homogenizer, USA) at 3000 rpm for 30 s. The mixture was then centrifuged at 6000 rpm for 10 min at room temperature. The resulting supernatant (150 µL) was removed and 1200 µL of Lowry B reagent was added and allowed to stand for 10 min at room temperature. Next, 150 µL of Lowry A reagent was added to the mixture, which was then homogenized and left for 20 min. A bluish color change was observed, and the absorbance was assessed at 600 nm using a UV-VIS spectrophotometer (UV-Vis 752N, China). Bovine serum albumin (BSA) was used as the standard.

2.5.3 Hydroxyproline level evaluation

The wound tissue underwent hydrolysis with 6N HCl at 130 °C for 4 h, was neutralized to pH 7 using Chloramine-T Oxidan, and was let to stand for 20 min at ambient temperature. The reaction was stopped by the addition of 0.4 M perchloric acid. Ehrlich's reagent was then added to the solution and incubated for 90 min at 60 °C. The absorbance was quantified at 557 nm using a spectrophotometer (UV-Vis 752N, China). A standard curve was established using hydroxyproline levels of 0, 6.3, 12.5, 25, 50, 100, 200, and 400 µg/mL, according to the same methodology used for wound tissue samples [25].

2.5.4 Total DNA Measurement

Skin tissue (0.05 g) taken from the wound area was placed in a tube containing 200 µL PBS and homogenized at 3000 rpm for 30 s. DNA was extracted using a Universal DNA Extraction Kit (D2100, Solarbio, Beijing) was used. Following the DNA extraction process, the total DNA content was measured using the Qubit™ dsDNA Quantification Assay Kit (catalog number: Q32851, Thermo Fisher Scientific, USA) and determined using the Invitrogen Qubit 4 Fluorometer (Thermo Fisher Scientific, USA) [25].

2.5.5 Histology Preparations

Mouse wound skin tissue was collected on day 10th to prepare histological specimens. Histological analysis was performed following the Parafin method and hematoxylin and eosin staining. Histological observations were performed under a light microscope at 100X magnification (Zeiss Primo Star, Germany). The number of fibroblasts was scored based on a previous study [26].

2.6 Data analysis

The characterization data of M-AgNPs were analyzed using graphs and photographs. Simultaneously, quantitative data derived from incision wound closure, protein concentrations, hydroxyproline levels, total DNA, and fibroblast counts were analyzed using the SPSS (Statistical Product and Service Solutions) Programme. ANOVA was performed using SPSS version 22 (SPSS, Inc., Chicago, IL, USA) to evaluate the significant variations among the treatment groups. Following the identification of significant differences using ANOVA, Duncan's multiple range test (DMRT) was performed. Statistical significance was assessed at a threshold of *p*-value<*0.05*.

3 Results and Discussion

3.1 *Green synthesizes of M-AgNPs*

The utilization of biological systems, particularly plant extracts, for the eco-friendly synthesis of nanoparticles, is an emerging domain in nanotechnology. Various plant extracts and techniques have been used to determine the benefits of these nanoparticles. In the medical field, specifically in wound-healing research, the use of plant extracts for nanoparticle production is a cost-effective and environmentally sustainable method. This study aimed to investigate the efficacy of silver nanoparticles (AgNPs) synthesized from the ethanolic extract of bulbs of *Myrmecodia* sp. in promoting wound healing in mouse models.

Upon introducing *Myrmecodia* sp. bulb extract to AgNO$_3$, the solution exhibited a noticeable change in color. The reaction started with a solution of pale brown hue. The solution became progressively darker after 30 min of continuous stirring. The color shift during the biogenesis of nanoparticles serves as a signal for the synthesis of M-AgNPs. Anju *et al*., [27] reported similar results, stating that the hue shift may be used to visually validate the formation of AgNPs using green synthesis. This color change occurs because of the conversion of silver ions (Ag$^+$) into silver nanoparticles [28], which is aided by the presence of bioactive phytochemicals in the bulb ethanolic extract of *Myrmecodia* sp. (Figure 2).
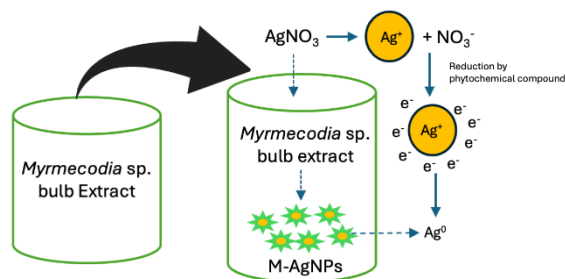
Figure 2: A reaction mechanism for the reduction of Ag+ to Ag0 by bioactive compounds from the bulb ethanolic extract of *Myrmecodia* sp.

Additionally, the Tyndall effect was used to validate the biosynthesis of M-AgNPs. Figures 3(a) (bulb ethanolic extract) and Figures 3(c) (AgNO$_3$) illustrate the early solutions, which exhibited little light dispersion. Nevertheless, the solution containing colloidal M-AgNPs (Figure 3(b)) exhibited the Tyndall effect as a beam of light was observed from the lateral perspective. This was attributed to the existence of lyophobic sol particles, which were sufficient for light dispersion, and indicated that M-AgNPs existed as colloidal particles in the ethanolic solution [29]. The Tyndall effect is particularly applicable to colloidal suspensions at room temperature, resulting in the rapid formation of M-AgNPs with a light brown hue.
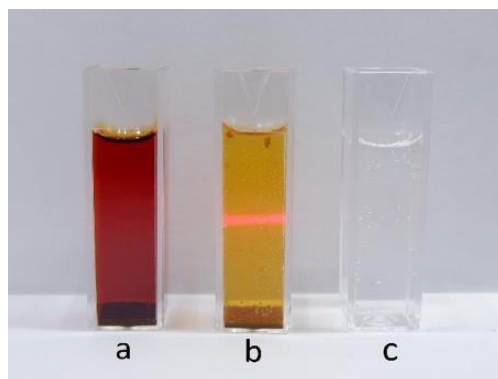
Figure 3: Tyndall effect of the AgNPs, biosynthesize using bulb ethanolic extract of *Myrmecodia* sp.

3.2 *M-AgNPs analysis using UV-Vis Spectrophotometer*

An absorption peak of M-AgNPs was observed at 460 nm (2.65 nm) in the UV-visible absorption spectra. In contrast, the ethanolic extract of *Myrmecodia* sp. bulb absorbed light at 489 nm with an absorbance of 2.80 (Figure 4). Furthermore, prior studies on AgNPs have shown that the absorption of light at approximately 460 nm using a UV-VIS spectrophotometer is a characteristic feature of these valuable metal particles [30]. The presence of a faint brown tint in the colloidal solutions at 460 nm suggests the retention of M-AgNPs owing to surface plasmon resonance (SPR), which helps stabilize the particles. The interaction occurs at a certain wavelength of visible light (400 and 500 nm), leading to the development of a brown hue in the solution, indicating the production of AgNPs [31], which is related to the surface plasmon resonance of AgNPs [32].
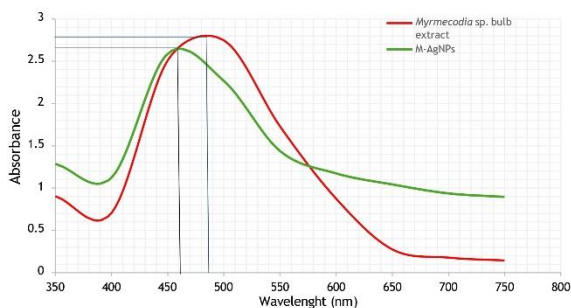
Figure 4: UV-VIS spectral of M-AgNPs and *Myrmecodia* sp. ethanolic bulb extract.

3.3 *M-AgNPs morphology and size using SEM*

Based on the characterization results obtained using SEM, it was determined that the nanocubes were in the form of M-AgNPs with an average particle size of 805 nm (Figure 5). In general, the current finding is in accordance with a previous study stating that nanoparticles have a size between 10–1000 nm [33].

A previous study conducted by Chaudhari and Ingale [34] reported that transmission electron microscopy (TEM) analysis of silver nanoparticles (AgNPs) synthesized using *Syzygium aromaticum* crude clove extract revealed the presence of nanoparticles with a nanocube shape and average size ranging from 80 to 150 nm. Other studies have

reported that AgNPs generated from plant extracts may have various forms, such as spherical, amorph, and round. The size of silver nanoparticles produced using plant extracts also has a wide range from one study to another [35]. Size variation is affected by phytochemical concentration and other synthesis parameters and conditions. Thus, the characteristics of AgNPs are determined by their size and form, which makes them extensively used in therapeutic applications.
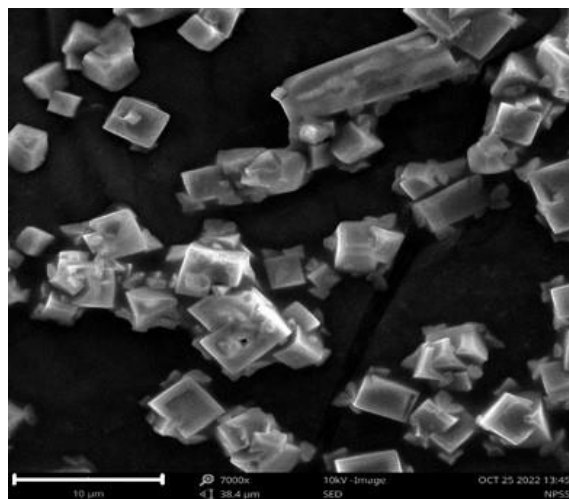
Figure 5: Scanning electron microscope of silver nanoparticle, biosynthesize using ethanolic extract of *Myrmecodia* sp. bulb.

3.4 *XRD characterization*

The synthesis of M-AgNPs from the ethanolic bulb extract was characterized using an XRD instrument to confirm the formation of nanoparticles with silver compound content as a specific metal [36]. The XRD analysis of the biosynthesized M-AgNPs confirmed their crystalline nature, indicating that they possessed a face-centered cubic structure. The purpose of the XRD characterization was to analyze the crystallinity of M-AgNPs and identify the Miller index value and crystallite size [37]. The characterization also aimed to determine the diffractogram pattern of the M-AgNPs synthesized from the bulb extract of *Myrmecodia* sp. The XRD instrument was used to ensure the formation of nanoparticle synthesis of AgNPs with silver compound content as a specific metal [36].
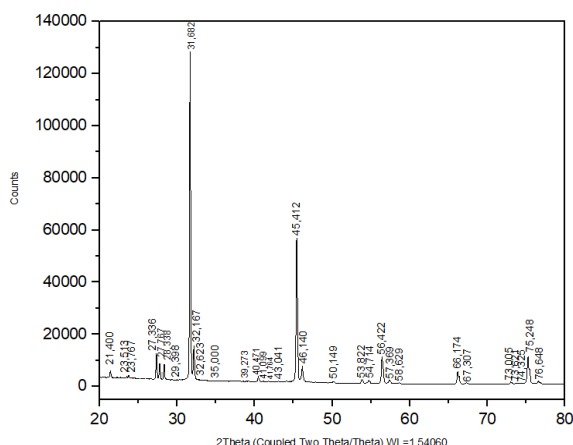
Figure 6: X-ray diffraction of M-AgNPs biosynthesized using ethanolic extract of *Myrmecodia* sp. bulb.

Based on the XRD diffractogram of M-AgNPs (Figure 6), M-AgNPs showed 2 theta diffraction intense peaks at 31.682°and 45.412°. The analysis also revealed diffraction peaks from 21.400° to 76.648°, confirming the crystallinity of M-AgNPs. These peaks correspond to metallic silver planes (e.g., 111 and 200), as reported by Fatimah *et al*., [37]. FTIR analysis further identified functional groups such as hydroxyl (O-H), carbonyl (C=O), and flavonoid-related bonds, which serve as reducing and stabilizing agents during nanoparticle synthesis. Furthermore, the peaks at approximately 31.682°, 45.412°, 67.301°, and 76.648° may also correspond to AgNPs crystallinity.

3.5　*FTIR spectroscopy*

FTIR analysis was used to determine the biomolecules that encapsulated and augmented the stability of the metal nanoparticles synthesized from the ethanolic extract of *Myrmecodia* sp. bulbs (Figure 7). The plant extract exhibited dual functionality as a reducing and capping agent, with the presence of specific functional groups verified by FTIR analysis of the M-AgNPs. The transmittance percentage curve of the IR spectrum was in the range of 500–4000 cm^{-1}.

The FTIR analysis of M-AgNPs showed the presence of C-H (aliphatic) groups at wavelengths 2917.82 cm^{-1}; 2849.56 cm^{-1}; and 1196.63 cm^{-1}, C-H (alkane) group at wavelength 1441.27 cm^{-1}, C=C (alkene) group 1601.85 cm^{-1}, C=C (benzene) group 765.03 cm^{-1}, C-O (alcohol) group at wave number

1279.68 cm^{-1} and C-O (flavonoid) group at wave number 1035.06 cm^{-1}.

The functional groups that indicate the presence of flavonoid compounds are C=C, C=O, C-O, C-H–H, and O-H single bonds [38]. The hydroxyl group (O-H) is one of the groups that participate in the process of reducing Ag+ ions into M-AgNPs [39]. According to Uddin *et al*., [40], bioactive compounds such as flavonoids, terpenoids, and coumarins, when interacting with Ag^+ ions, lead to the formation of AgNPs. Flavonoids act as reductants and stabilizers because they contain hydroxyl groups (O-H), form an electric double layer, and can interact with silver particles [41].
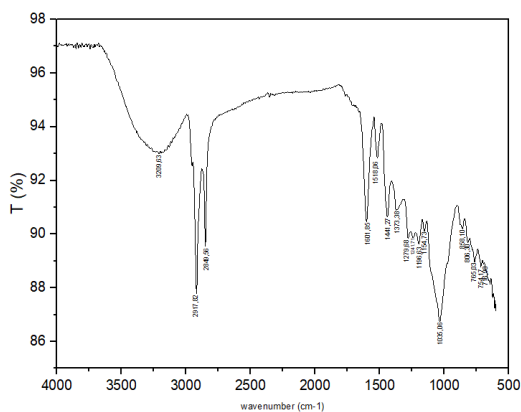
Figure 7: FTIR spectra of the *Myrmecodia* sp. ethanolic bulb extract in synthesizing silver nanoparticles.

3.6　*In vivo test*

The enclosure of incision wounds occurred most quickly in mice group P5 (20% M-AgNPs ointment) on day 12th with a percentage value of 100.00 ± 0% (Table 2). On the day 15th, all mice in the treatment groups either treated with *Myrmecodia* sp. bulb extract ointment (P1, P2, and P3), M-AgNPs ointment (P4, P5, and P6) or vaseline (K+Pov) had a percentage value of 100.00 ± 0.00 In contrast, to the K-group (percentage value 97.50 ± 0.86) and K+Vas (percentage value 98.75 ± 0.94), mice still had wounds that have not healed, indicating slow wound closure rate compared to others.

Mice in the K- group were not administered any treatment, and the wound was left open, allowing the wound to be infected by germs or bacteria, causing relatively longer wound healing [42]. In the wound healing process, the K+Vas group administered

Vaseline only acts as a wound cover and does not have a wound healing effect; however, it functions in maintaining skin moisture and as an emollient that may hydrate the skin. Vaseline can remain on the skin for a long time, does not easily evaporate into the air, and is not easily washed, thus prolonging the contact of the drug with the skin [43]. The administration of povidone iodine to mice in the K+Pov group on day 15 resulted in a completely closed wound, while K+Vas had a longer wound closure process. The wound closure process was faster in the K+Pov group than in the K- group. This finding is due to povidone iodine 10% works as an antimicrobial to accelerate wound healing, but it has side effects that cause irritation, hypersensitivity (allergies), and leave residue [44].

Table 2: Wound enclosure percentage (%) of mice during M-AgNPs treatment for 15 days.

Groups	Wound enclosure percentage (%)					
	0	3	6	9	12	15
K-	$_1$0.00±0.00^a	$_1$9.50±5.48^a	$_2$39.75±3.75^a	$_3$63.50±4.90^a	$_4$83.50±3.27^a	$_5$97.50±0.86^a
K+Vas	$_1$0.00±0.00^a	$_1$18.50±7.35^a	$_3$47.25±3.75^{ab}	$_3$63.50±4.90^a	$_4$90.50±2.46^a	$_5$98.75±0.94^{ab}
K+Pov	$_1$0.00±0.00^a	$_2$18.50±7.35^a	$_4$57.00±7.00^{bcd}	$_4$81.75±2.25^b	$_5$97.50±0.86^b	$_6$100.00±0.00^{bc}
P1	$_1$0.00±0.00^a	$_2$22.75±8.57^a	$_3$63.50±4.90^{bcd}	$_4$87.50±2.02^b	$_5$98.75±0.94^{bc}	$_5$100.00±0.00^{bc}
P2	$_1$0.00±0.00^a	$_2$18.50±7.35^a	$_3$50.50±5.72^{abc}	$_4$83.50±3.27^b	$_5$99.50±0.28^{bc}	$_5$100.00±0.00^{bc}
P3	$_1$0.00±0.00^a	$_2$35.50±6.53^a	$_3$66.25±5.70^{cb}	$_4$85.25±3.79^b	$_5$98.75±0.94^{bc}	$_5$100.00±0.00^{bc}
P4	$_1$0.00±0.00^a	$_2$22.75±8.57^a	$_3$50.50±5.72^{abc}	$_4$85.25±3.79^b	$_5$98.75±0.94^{bc}	$_5$100.00±0.00^{bc}
P5	$_1$0.00±0.00^a	$_2$35.50±6.53^a	$_3$69.50±3.17^d	$_4$95.50±1.65^c	$_5$100.00±0.00^c	$_5$100.00±0.00^{bc}
P6	$_1$0.00±0.00^a	$_2$18.50±7.35^a	$_3$50.50±5.72^{abc}	$_4$81.25±3.88^b	$_5$98.50±0.86^{bc}	$_6$100.00±0.00^{bc}

Note: K- (no treatment), K+Vas (Vaseline base ointment), K+Pov (povidone iodine ointment), P1–P3 (With 10, 20, and 30% *Myrmecodia* sp. bulb ethanolic extract ointment), P4–P6 (With 10, 20, and 30% M-AgNPs ointment). Mean ± SE values followed by superscript letters (a-d) differing in the same column and subscript numbers (1–6) differing in the same row indicate significant differences (p-value<0.05).

Furthermore, the healing of mouse incision wounds in the treatment group given M-AgNP ointment, especially at concentrations of 20% and 30%, had a faster wound closure process compared to the extract ointment concentrations of 10%, 20%, and 30%. According to previous research [45]: the use of M-AgNPs ointment can cause a quicker decrease in wound area than in other groups, considering its significance in the wound healing process. M-AgNPs can act as antibacterial agents to inhibit bacterial replication by releasing silver ions that can damage bacterial RNA and DNA and suppress bacterial growth, causing a faster wound healing process [46]. M-AgNPs can maintain the release of silver ions, thus prolonging the treatment effect and minimizing toxicity [47].

The M-AgNPs ointment with 20% concentration was more effective in wound closure than the M-AgNPs ointment with 10% concentration or the M-AgNPs ointment with 30% concentration. According to Hayouni *et al.*, [48], ointment formulations with low extract concentrations have a slower wound healing effect because there are few active substances. Meanwhile, Putrianirma *et al.*, [49] reported that high concentrations of the extract caused the ointment to block a wound that dried into a scab in the wound area. The wound resulted in longer inflammation, and wound healing was inhibited. The high flavonoid content of the extract may reduce its antioxidant properties [50].

Mice treated with 10, 20, or 30% *Myrmecodia* sp. the ethanolic bulb extract ointment showed faster wound healing than the K- and K+Vas groups. The present findings may be due to antioxidant compounds, such as alkaloids, saponins, flavonoids, and tannins, which are found in *Myrmecodia* sp. extract [51]. Both flavonoids and tannins play an active role in inhibiting and killing bacteria that can infect wounds, damage microsomes and lysosomes, and damage the permeability of bacterial cell walls, resulting in the interaction between flavonoids and bacterial DNA that can inhibit bacterial motility. Flavonoid compounds in the *Myrmecodia* sp. extract also play a role in anti-inflammation, which may inhibit inflammatory mediators such as arachidonic acid, lipoxygenase (COX) enzymes, and cyclooxygenase (LO), reduce leukocyte accumulation, and offset free radical reactions [52]. Furthermore, flavonoids are also important in the process of reducing Ag^+ nanoparticles to Ag^0 [53], and improving blood circulation throughout the body, preventing blockage of blood vessels, and reducing pain due to swelling or bleeding. Tannin compounds also act as antibacterial, antifungal, and astringent agents for shrinking skin pores, hardening skin, and stopping mild bleeding. Saponin compounds, which are also found in *Myrmecodia* sp. the ethanolic bulb extract functions as an antiseptic to kill germ cells and prevent the growth of microorganisms in wounds [54].

Table 3: Mean ± SE of protein, hydroxyproline level, total DNA, and fibroblast scoring of wound skin tissue of mice treated with various ointments.

Groups	Protein Level µg/mL	Hidroksiprolin Level µg/mL	Total DNA (µg/mL)	Fibroblast Scoring
K-	1409.37±29.93[e]	4118.74±33.63[b]	7.02±0.31[g]	1.87±0.00[b]
K+Vas	1301.25±31.70[de]	4191.24±47.82[b]	5.48±0.14[f]	1.87±0.00[b]
K+Pov	1245.31±34.34[d]	4210.83±33.90[b]	4.59±0.22[e]	1.79±0.072[b]
P1	950.00±52.32[c]	3867.91±27.99[a]	3.51±0.25[d]	1.79±0.072[b]
P2	861.62±11.66[bc]	3789.58±39.85[a]	2.11±0.05[bc]	1.72±0.083[ab]
P3	885.93±14.12[bc]	3801.66±46.19[a]	2.44±0.17[c]	1.75±0.083[ab]
P4	880.93±36.26[bc]	3799.99±16.37[a]	2.15±0.10[bc]	1.58±0.00[a]
P5	721.25±66.28[a]	3782.91±37.22[a]	1.29±0.49[a]	1.58±0.00[a]
P6	780.00±39.65[ab]	3783.75±23.68[a]	1.62±0.20[ab]	1.58±0.00[a]

Note: K- (no treatment), K+Vas (Vaseline base ointment), K+Pov (povidone iodine ointment), P1–P3 (With 10, 20, and 30% *Myrmecodia* sp. bulb ethanolic extract ointment), P4–P6 (With 10, 20, and 30% M-AgNPs ointment). Mean ± SE values followed by different superscript letters (a–g) in the same column indicate significant differences (*p*-value<0.05).

Based on the measurement of protein levels, hydroxyproline levels, total DNA content, and the number of fibroblasts in mice skin tissue (Table 3), the mice treated with 20% M-AgNPs ointment (Group P5) had the lowest level of protein levels (721.250 ± 66.28 µg/mL), hydroxyproline levels (3782.915 ± 37.221 µg/mL), total DNA values (1.297 ± 0.496 µg/mL), and the number of fibroblasts of (1.581 ± 0.00). Meanwhile, mice in group K- was the group that had the highest values of protein levels (1409.375 ± 29.937 µg/mL), hydroxyproline levels (4118.747 ± 33.632 µg/mL), total DNA (7.020 ± 0.318 µg/mL), and the number of fibroblasts (1.870 ± 0.000 µg/mL). Measurement of protein levels, hydroxyproline levels, and total DNA of mouse skin tissue was carried out on day 10 because there were mice in group P5 (given 20% M-AgNPs ointment) that showed more than 50% of the population of mice in the wound healing condition.

Histological preparations (Figure 8) were analyzed using a scoring method to calculate the number of fibroblasts. After scoring the number of fibroblasts, the K- and K+Vas groups showed the highest number of fibroblasts. Group P5 mice (20% M-AgNPs ointment) had the lowest number of fibroblasts, followed by P4 mice (10% M-AgNPs ointment), P6 (30% M-AgNPs ointment), P2 (20% extract ointment), and P3 (30% extract ointment), which had the number of fibroblasts with no significant difference from group P5 mice.

These results revealed that on day 10, mice in K- and K+Vas groups were still in the proliferation phase. The proliferation phase is indicated by the number of fibroblasts that continue to increase during this phase [55]. Meanwhile, P5 mice, which had the lowest number of fibroblasts, were in the final phase of proliferation and entered the remodeling phase.

This is in accordance with the results of Darby *et al.*, [56], who found that, at the end of the proliferation phase, the number of fibroblast cells decreased upon entering the remodeling phase. The rapid fibroblast proliferation process makes fibroblast elimination work faster, indicating wound healing [57]. In addition, M-AgNPs may release silver ions that inhibit microbial growth, reduce inflammation, and promote fibroblast proliferation.

The proliferation phase of wound healing is characterized by cell division (cell proliferation). Increased cell division causes an increase in DNA and protein content [58]. The proliferation phase also exhibits protein synthesis activity in the skin, namely collagen produced by fibroblasts in large quantities [59]. Fibroblasts are stem cells that play a role in the formation of collagen fibers in the matrix. Collagen fibers provide the strength and integrity to link the wound so that they heal properly and quickly. In addition, fibroblasts influence the re-epithelialization process, which completely closes the wound [60]. The collagen synthesis activity of fibroblasts and the synthesis of hydroxyproline, a basic component of intracellular collagen, increase during wound healing.

4 Conclusions

The bulb of *Myrmecodia* sp. served as a reducing agent for the synthesis of M-AgNPs. The occurrence of a hue shift and the Tyndall effect indicated the effective production of M-AgNPs. The surface plasmon resonance of the M-AgNPs was detected at 460 nm, indicating an ideal peak. FTIR analysis identified several phytochemically active groups in M-AgNPs. Furthermore, SEM examination indicated that the M-AgNPs were comprised of nanocube particles measuring 805 nm. The study demonstrated

that the closure of incision wounds transpired more rapidly in mice administered 20% M-AgNPs ointment by the 12th day. The animals administered the 20% M-AgNPs ointment had the lowest levels of protein, hydroxyproline, total DNA content, and fibroblast count in their skin tissue. The M-AgNPs produced offer a direct approach to the synthesis of AgNPs from a technological perspective. This technology has numerous advantages, including cost-effectiveness, suitability for medical and pharmaceutical applications, and the capacity for large-scale commercial production. The current study indicates that AgNPs synthesized using *Myrmecodia* sp. ethanolic bulb extract can be used as a wound healing agent, addressing the demand for sustainable biomedical solutions in healthcare.
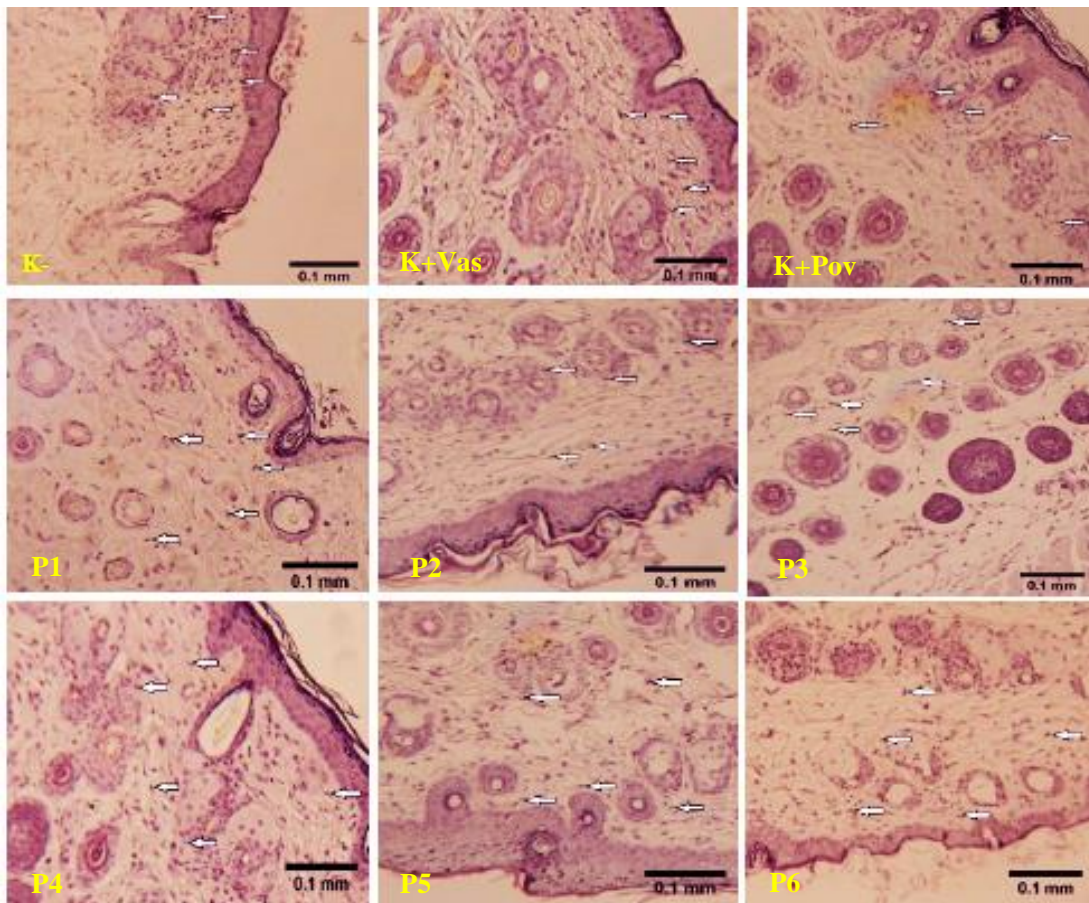
Figure 8: Fibroblast of wound mice skin tissue in various treatment groups, Note: K- (no treatment), K+Vas (Vaseline base ointment), K+Pov (Povidone iodine ointment), P1–P3 (With 10, 20, and 30% *Myrmecodia* sp. bulb ethanolic extract ointment), P4–P6 (With 10, 20, and 30% M-AgNPs ointment), fibroblasts (white arrows). Haematoxylin and eosin staining with 100X magnification.

Author Contributions

R.A., M.W., and R.A.N.: Conceptualization and Resources; R.A., R.A.N., and H.M.: Conception of the article, formal analysis, validation, drafting (Writing-original Draft Preparation), and review (Writing-Review and Editing), performed critical revisions related to important intellectual content of the

manuscript; R.A., M.W., and R.A.N. contributed to the final revision of the manuscript; R.A., R.A.N., H.M., and E.M.: performed data curation, project administration, Supervision, Software operation, and Methodology; R.A., R.A.N., R.R.: Investigation and project administration. All authors have read and agreed to the published version of the manuscript.

Conflicts of Interest

The authors declare no conflict of interest.

Ethical Statement

Animal ethics were approved (No. 05/KEPK-FK/I/2023) by the Ethics Committee for Health Research, Faculty of Medicine, Mulawarman University, Samarinda, Indonesia, for the use of mice (72 mice) in the in vivo wound healing experiment. This research was conducted in accordance with ARRIVE standards.

References

[1] A. Meher, A. Tandi, S. Moharana, S. Chakroborty, S. S. Mohapatra, A. Mondal, S. Dey, and P. Chandra, "Silver nanoparticle for biomedical applications: A review," *Hybrid Advances*, vol. 6, 2024, Art. no. 100184, doi: j.hybadv.2024.100184.

[2] A. Puri, P. Mohite, S. Maitra, V. Subramaniyan, V. Kumarasamy, D. E. Uti, A. A. Sayed, F. M. El-Demerdash, M. Alqahtani, and A. F. El-Kott, "From nature to nanotechnology: The interplay of traditional medicine, green chemistry, and biogenic metallic phytonanoparticles in modern healthcare innovation and sustainability," *Biomedicine and Pharmacotherapy*, vol. 170, 2024, Art. no. 116083, doi: 10.1016/j.biopha. 2023.116083.

[3] M. Qubtia, S. A. Ghumman, S. Noreen, H. Hameed, S. Noureen, R. Kausar, A. Irfan, P. Akhtar Shah, H. Afzal, and M. Hameed, "Evaluation of plant-based silver nanoparticles for antioxidant activity and promising wound-healing applications," *ACS Omega*, vol. 9, no. 10, pp. 12146–12157, 2024.

[4] J. Horne, C. D. Bleye, P. Lebrun, K. Kemik, T. V. Laethem, P.-Y. Sacré, P. Hubert, C. Hubert, and E. Ziemons, "Optimization of silver nanoparticles synthesis by chemical reduction to enhance sers quantitative performances: Early characterization using the quality by design approach," *Journal of Pharmaceutical and Biomedical Analysis*, vol. 233, 2023, Art. no. 115475, doi: 10.1016/j.jpba.2023.115475.

[5] P. K. Dikshit, J. Kumar, A. K. Das, S. Sadhu, S. Sharma, S. Singh, P. K. Gupta, and B. S. Kim, "Green synthesis of metallic nanoparticles: Applications and limitations," *Catalysts*, vol. 11, no. 8, p. 902, 2021.

[6] K. N. Thakkar, S. S. Mhatre, and R. Y. Parikh, "Biological synthesis of metallic nanoparticles," *Nanomedicine: Nanotechnology, Biology and Medicine*, vol. 6, no. 2, pp. 257–262, 2010.

[7] N. M. Ishak, S. Kamarudin, and S. Timmiati, "Green synthesis of metal and metal oxide nanoparticles via plant extracts: An overview," *Materials Research Express*, vol. 6, no. 11, pp. 1–14, 2019.

[8] F. Trotta, A. Dony, M. Mok, A. Grillo, T. Whitehead-Clarke, S. Homer-Vanniasinkam, and A. Kureshi, "In vitro characterization of bionanocomposites with green silver nanoparticles: A step towards sustainable wound healing materials," *Nano Select*, vol. 5, no. 2, pp. 1–14, 2023.

[9] H. Achmad, S. Horax, S. Ramadhany, H. Handayani, R. Pratiwi, S. Oktawati, N. Faizah, and M. Sari, "Resistivity of ant nest (*myrmecodia pendans*) on ethanol fraction burkitt's lymphoma cancer cells (invitro) through interleukin 8 angiogenesis obstacles (il-8)," *Journal of International Dental and Medical Research*, vol. 12, no. 2, 2019.

[10] J. Sudiono, C. T. Oka, and P. Trisfilha, "The scientific base of *myrmecodia pendans* as herbal remedies," *British Journal of Medicine and Medical Research*, vol. 8, no. 3, pp. 230–237, 2015.

[11] R. A. Nugroho, R. Aryani, H. Manurung, Y. P. Sari, and R. Rudianto, "*Myrmecodia pendens* bulb extract in the lele dumbo (*clarias gariepinus*) feed: Effects on the growth performance, survival, and blood indices," *Journal of Aquaculture and Fish Health*, vol. 11, no. 1, pp. 21–36, 2022.

[12] N. P. Hanh, N. H. T. Phan, N. T. D. Thuan, T. T. H. Hanh, L. T. Vien, N. P. Thao, N. V. Thanh, N. X. Cuong, N. Q. Binh, N. H. Nam, P. V. Kiem, Y. H. Kim, and C. V. Minh "Two new simple iridoids from the ant-plant *Myrmecodia*

tuberosa and their antimicrobial effects," *Natural Product Research*, vol. 30, no.18, pp. 2071–2076, 2016, doi: 10.1080/14786419.2015. 1113412.

[13] A. Oliveira, S. Simões, A. Ascenso, and C. P. Reis, "Therapeutic advances in wound healing," *Journal of Dermatological Treatment*, vol. 33, no. 1, pp. 2–22, 2022, doi: 10.1080/09546634. 2020.1730296.

[14] S. L. Percival, D. Williams, T. Cooper, and J. Randle, *Biofilms in Infection Prevention and Control: A Healthcare Handbook*. New York: Academic Press, pp. 127–139, 2014.

[15] J. D. Jones, H. E. Ramser, A. E. Woessner, and K. P. Quinn, "In vivo multiphoton microscopy detects longitudinal metabolic changes associated with delayed skin wound healing," *Communications Biology*, vol. 1, 2018, Art. no. 198, doi: 10.1038/s42003-018-0206-4.

[16] Y. Dutt, R. P. Pandey, M. Dutt, A. Gupta, A. Vibhuti, V. S. Raj, C.-M. Chang, and A. Priyadarshini, "Silver nanoparticles phytofabricated through *Azadirachta indica*: Anticancer, apoptotic, and wound-healing properties," *Antibiotics*, vol. 12, no. 1, 2023, doi: 10.3390/antibiotics12010121.

[17] N. Assad, M. Naeem-ul-Hassan, M. A. Hussain, A. Abbas, M. Sher, G. Muhammad, Y. Assad, and M. Farid-ul-Haq, "Diffused sunlight assisted green synthesis of silver nanoparticles using *Cotoneaster nummularia* polar extract for antimicrobial and wound healing applications," *Natural Product Research*, pp. 1–15, 2023, doi: 10.1080/14786419.2023.2295936.

[18] A. H. Al-Nadaf, A. Awadallah, and S. Thiab, "Superior rat wound-healing activity of green synthesized silver nanoparticles from acetonitrile extract of *Juglans regia* L: Pellicle and leaves," *Heliyon*, vol. 10, no. 2, 2024, doi: 10.1016/ j.heliyon.2024.e24473.

[19] R. Z. Maarebia, A. W. Wahab, and P. Taba, "Synthesis and characterization of silver nanoparticles using water extract of sarang semut (*Myrmecodia pendans*) for blood glucose sensors," *Jurnal Akta Kimia Indonesia (Indonesia Chimica Acta)*, vol. 12, no. 1, pp. 29–46, 2019, doi: 10.20956/ica.v12i1.5881.

[20] V. Kalynovskyi, O. Smirnov, P. Zelena, Y. Yumyna, M. Kovalenko, V. Dzhagan, M. Dzerzhynsky, and N. Taran, "Biosynthesis of silver nanoparticles with antioxidant and

bactericidal activities using *Capsicum annuum* fruit extract," *Regulatory Mechanisms in Biosystems*, vol. 14, no. 3, pp. 393–398, 2023, doi: 10.15421/ 022358.

[21] H. Barabadi, F. Mojab, H. Vahidi, B. Marashi, N. Talank, O. Hosseini, and M. Saravanan, "Green synthesis, characterization, antibacterial and biofilm inhibitory activity of silver nanoparticles compared to commercial silver nanoparticles," *Inorganic Chemistry Communications*, vol. 129, 2021, Art. no. 108647, doi: 10.1016/j.inoche. 2021.108647.

[22] R. Aryani, R. A. Nugroho, H. Manurung, R. Mardayanti, R. Rudianto, W. Prahastika, A. Auliana, and A. P. B. Karo, "*Ficus deltoidea* leaves methanol extract promote wound healing activity in mice," *EurAsian Journal of Biosciences*, vol. 14, pp. 85–91, 2020.

[23] B. Tekleyes, S. A. Huluka, K. Wondu, and Y. T. Wondmkun, "Wound healing activity of 80% methanol leaf extract of *Zehneria scabra* (L.f) Sond (cucurbitaceae) in mice," *Journal of experimental pharmacology*, vol. 13, pp. 537–544, 2021, doi: 10.2147/JEP.S303808.

[24] J. H. Waterborg, "The lowry method for protein quantitation," in *the Protein Protocols Handbook*, Berlin, Germany: Springer Nature, pp. 7–10, 2009.

[25] R. A. Nugroho, R. Aryani, H. Manurung, R. Rudianto and D. Prameswari, "Wound healing potency of *Terminalia catappa* in mice (*Mus musculus*)," *EurAsian Journal of BioSciences*, vol. 13, no. 2, pp. 2337–2342, 2019.

[26] M. Karimi, P. Parsaei, S. Y. Asadi, S. Ezzati, R. K. Boroujeni, A. Zamiri, and M. Rafieian-Kopaei, "Effects of *Camellia sinensis* ethanolic extract on histometric and histopathological healing process of burn wound in rat," *Middle East Journal of Scientific Research*, vol. 13, no. 1, pp. 14–19, 2013.

[27] T. R. Anju, S. Parvathy, M. V. Veettil, J. Rosemary, T. H. Ansalna, M. M. Shahzabanu, and S. Devika, "Green synthesis of silver nanoparticles from *Aloe vera* leaf extract and its antimicrobial activity," *Materials Today: Proceedings*, vol. 43, pp. 3956–3960, 2021, doi: 10.1016/j.matpr.2021.02.665.

[28] F. Mohammadi, M. Yousefi, and R. Ghahremanzadeh, "Green synthesis, characterization and antimicrobial activity of silver nanoparticles (AgNPs) using leaves and

stems extract of some plants," *Advanced Journal of Chemistry-Section A*, vol. 2 no. 4, pp. 266–275, 2019, doi: 10.33945/SAMI/AJCA.2019.4.1.

[29] A. John, A. Shaji, K. Velayudhannair, M. Nidhin, and G. Krishnamoorthy, "Anti-bacterial and biocompatibility properties of green synthesized silver nanoparticles using *Parkia biglandulosa* (Fabales: Fabaceae) leaf extract," *Current Research in Green and Sustainable Chemistry*, vol. 4, 2021, Art. no. 100112, doi: 10.1016/j.crgsc.2021.100112.

[30] A. R. Vilchis-Nestor, V. Sánchez-Mendieta, M. A. Camacho-López, R. M. Gómez-Espinosa, M. A. Camacho-López, and J. A. Arenas-Alatorre, "Solventless synthesis and optical properties of au and ag nanoparticles using *Camellia sinensis* extract," *Materials letters*, vol. 62, no. 17–18, pp. 3103–3105, 2008, doi: 10.1016/j.matlet.2008.01.138.

[31] S. Kumar, S. Taneja, S. Banyal, M. Singhal, V. Kumar, S. Sahare, S.-L. Lee, and R. K. Choubey, "Bio-synthesised silver nanoparticle-conjugated l-cysteine ceiled mn: Zns quantum dots for eco-friendly biosensor and antimicrobial applications," *Journal of Electronic Materials*, vol. 50, pp. 3986–3995, 2021, doi: 10.1007/s11664-021-08926-4.

[32] M. M. Martin and R. E. Sumayao Jr, "Facile green synthesis of silver nanoparticles using *Rubus rosifolius* linn aqueous fruit extracts and its characterization," *Applied Science and Engineering Progress*, vol. 15, no. 3, 2022, doi: 10.14416/j.asep.2021.10.011.

[33] E. Wu, Y. Li, Q. Huang, Z. Yang, A. Wei, and Q. Hu, "Laccase immobilization on amino-functionalized magnetic metal organic framework for phenolic compound removal," *Chemosphere*, vol. 233, pp. 327–335, 2019, doi: 10.1016/j.chemosphere.2019.05.150.

[34] A. N. Chaudhari and A. G. Ingale, "*Syzygium aromaticum* extract mediated, rapid and facile biogenic synthesis of shape-controlled (3D) silver nanocubes," *Bioprocess and Biosystems Engineering*, vol. 39, pp. 883–891, 2016. doi: 10.1007/s00449-016-1567-z.

[35] M. Sharifi-Rad, H. S. Elshafie, and P. Pohl, "Green synthesis of silver nanoparticles (agnps) by *Lallemantia royleana* leaf extract: Their bio-pharmaceutical and catalytic properties," *Journal of Photochemistry and Photobiology A:* *Chemistry*, vol. 448, 2024, Art. no. 115318, doi: 10.1016/j.jphotochem.2023.115318.

[36] M. A. Alqahtani, M. R. Al Othman, and A. E. Mohammed, "Bio fabrication of silver nanoparticles with antibacterial and cytotoxic abilities using lichens," *Scientific Reports*, vol. 10, no. 1, 2020, doi: 10.1038/s41598-020-73683-z.

[37] S. Fatimah, R. Ragadhita, D. F. Al Husaeni, and A. B. D. Nandiyanto, "How to calculate crystallite size from x-ray diffraction (XRD) using scherrer method," *ASEAN Journal of Science and Engineering*, vol. 2, no. 1, pp. 65–76, 2022, doi: 10.17509/ajse.v2i1.37647.

[38] B. Yadav, R. K. Yadav, G. Srivastav, and R. Yadav, "Experimental raman, ftir and uv-vis spectra, DFT studies of molecular structures and conformations, barrier heights against internal rotations, thermodynamic functions and bioactivity of biologically active compound-isorhamnetin," *Polycyclic Aromatic Compounds*, vol. 44, no. 3, pp. 1609–1643, 2024, doi: 10.1080/10406638.2023.2201460.

[39] H. Peng, H. Guo, P. Gao, Y. Zhou, B. Pan, and B. Xing, "Reduction of silver ions to silver nanoparticles by biomass and biochar: Mechanisms and critical factors," *Science of The Total Environment*, vol. 779, 2021, Art. no. 146326, doi: 10.1016/j.scitotenv.2021.146326.

[40] I. Uddin, K. Ahmad, A. A. Khan, and M. A. Kazmi, "Synthesis of silver nanoparticles using *Matricaria recutita* (babunah) plant extract and its study as mercury ions sensor," *Sensing and Bio-Sensing Research*, vol. 16, pp. 62–67, 2017, doi: 10.1016/j.sbsr.2017.11.005.

[41] S. L. Ramírez-Rosas, E. Delgado-Alvarado, L. O. Sanchez-Vargas, A. L. Herrera-May, M. G. Peña-Juarez, and J. A. Gonzalez-Calderon, "Green route to produce silver nanoparticles using the bioactive flavonoid quercetin as a reducing agent and food anti-caking agents as stabilizers," *Nanomaterials*, vol. 12, no. 19, 2022, doi: 10.3390/nano12193545.

[42] T. Maheswary, A. A. Nurul, and M. B. Fauzi, "The insights of microbes' roles in wound healing: A comprehensive review," *Pharmaceutics*, vol. 13, no. 7, 2021, doi: 10.3390/pharmaceutics13070981.

[43] M. Kumar, U. K. Mandal, and S. Mahmood, *Dermatological Formulations, in Dosage Forms, Formulation Developments and*

Regulations. New York: Academic Press, pp. 613–642, 2024.

[44] K. Maliyar, A. Mufti, and R. G. Sibbald, "The use of antiseptic and antibacterial agents on wounds and the skin," in *Local Wound Care for Dermatologists*, Berlin: Germany: Springer Nature, pp. 35–52, 2020, doi: 10.1007/978-3-030-28872-3_5.

[45] N. Abbasi, H. Ghaneialvar, R. Moradi, M. M. Zangeneh, and A. Zangeneh, "Formulation and characterization of a novel cutaneous wound healing ointment by silver nanoparticles containing *Citrus lemon* leaf: A chemobiological study," *Arabian Journal of Chemistry*, vol. 14, no. 7, 2021, Art. no. 103246, doi: 10.1016/j.arabjc.2021.103246.

[46] A. Salleh, R. Naomi, N. D. Utami, A. W. Mohammad, E. Mahmoudi, N. Mustafa, and M. B. Fauzi, "The potential of silver nanoparticles for antiviral and antibacterial applications: A mechanism of action," *Nanomaterials*, vol. 10, no. 8, 2020, doi: 10.3390/nano10081566.

[47] B. Reidy, A. Haase, A. Luch, K. A. Dawson, and I. Lynch, "Mechanisms of silver nanoparticle release, transformation and toxicity: A critical review of current knowledge and recommendations for future studies and applications," *Materials*, vol. 6, no. 6, pp. 2295–2350, 2013, doi: 10.3390/ma6062295.

[48] E. A. Hayouni, K. Miled, S. Boubaker, Z. Bellasfar, M. Abedrabba, H. Iwaski, H. Oku, T. Matsui, F. Limam, and M. Hamdi, "Hydroalcoholic extract based-ointment from *Punica granatum* L. peels with enhanced in vivo healing potential on dermal wounds," *Phytomedicine*, vol. 18, no. 11, pp. 976–984, 2011, doi: 10.1016/j.phymed.2011.02.011.

[49] R. Putrianirma, N. Triakoso, M. N. Yunita, I. S. Yudaniayanti, I. S. Hamid, and F. Fikri, "Efektivitas ekstrak daun afrika (*Vernonia amygdalina*) secara topikal untuk reepitelisasi penyembuhan luka insisi pada tikus putih (*Rattus novergicus*)," *Jurnal Medika Veterinaria*, vol. 2, no. 1, pp. 30–35, 2019, doi: 10.20473/jmv.vol2.iss1.2019.30-35.

[50] I. M. Comino-Sanz, M. D. López-Franco, B. Castro, and P. L. Pancorbo-Hidalgo, "The role of antioxidants on wound healing: A review of the current evidence," *Journal of Clinical Medicine*, vol. 10, no. 16, 2021, doi: 10.3390/jcm10163558.

[51] M. Daulay, M. Syahputra, M. I. Sari, T. Widyawati, and D. R. Anggraini, "The potential of *Myrmecodia pendans* in preventing complications of diabetes mellitus as an antidiabetic and antihyperlipidemic agent," *Open Veterinary Journal*, vol. 14, no. 7, pp. 1607–1613, 2024, doi: 10.5455/OVJ.2024.v14.i7.10.

[52] J. H. Faleiro, R. C. Gonçalves, M. N. G. dos Santos, D. P. da Silva, P. L. F. Naves, and G. Malafaia, "The chemical featuring, toxicity, and antimicrobial activity of *psidium cattleianum* (myrtaceae) leaves," *New Journal of Science*, vol. 2016, no. 1, 2016, doi: 10.1155/2016/7538613.

[53] S. Bhattacharjee, C. Ghosh, A. Sen, and M. Lala, "Characterization of *Firmiana colorata* (roxb.) r. Br. Leaf extract and its silver nanoparticles reveal their antioxidative, anti-microbial, and anti-inflammatory properties," *International Nano Letters*, vol. 13, pp. 235–247, 2023, doi: 10.1007/s40089-023-00392-6.

[54] P. A Manar, S. E. P. Utama, G. M. Hasan, and M. S. Hidayat. "The potential of sarang semut (*Myrmecodia* spp) as medicinal plants," *IOP Conference Series: Earth and Environmental Science*, vol. 394, 2019, Art. no. 012032, doi: 10.1088/1755-1315/394/1/012032.

[55] C. Theoret and J. Schumacher, *Equine Wound Management*. New York: John Wiley and Sons, 2016.

[56] I. A. Darby, B. Laverdet, F. Bonté, and A. Desmoulière, "Fibroblasts and myofibroblasts in wound healing," *Clinical, Cosmetic and Investigational Dermatology*, vol. 7, pp. 301–311, 2014, doi: 10.2147/CCID.S50046.

[57] A. Stunova and L. Vistejnova, "Dermal fibroblasts—a heterogeneous population with regulatory function in wound healing," *Cytokine and Growth Factor Reviews*, vol. 39, pp. 137–150, 2018, doi: 10.1016/j.cytogfr.2018.01.003.

[58] M. P. Fara, S. Kakoolaki, A. Asghari, I. Sharifpour, and R. Kazempoor, "Review Article: Wound healing by functional compounds of Echinodermata, Spirulina and chitin products," *Sustainable Aquaculture and Health Management Journal*, vol. 6 no. 2, pp. 23–38, 2020, doi: 10.52547/ijaah.6.2.23

[59] L. R. L. Diniz, L. L. Calado, A. B. S. Duarte, and D. P. de Sousa, "*Centella asiatica* and its metabolite asiatic acid: Wound healing effects

and therapeutic potential," *Metabolites*, vol. 13, no. 2, 2023, doi: 10.3390/metabo13020276.

[60] V. A. S David, V. R. Güiza-Argüello, M. L. Arango-Rodríguez, C. L. Sossa, and S. M. Becerra-Bayona, "Decellularized tissues for wound healing: Towards closing the gap between scaffold design and effective extracellular matrix remodeling," *Frontiers in Bioengineering and Biotechnology*, vol. 10, 2022, doi: 10.3389/fbioe.2022.821852.